Half-Sandwich Manganese Complex Bearing Fused Oxazoline-NHC Ligand: Conformational Analysis and Evaluation in Asymmetric Ketone Hydrosilylation

Matthieu Cavailles, Oleg Filippov, Vincent César, Noël Lugan, Dmitry Valyaev

Half-Sandwich Manganese Complex Bearing Fused Oxazoline-NHC Ligand: Conformational Analysis and Evaluation in Asymmetric Ketone Hydrosilylation

Matthieu Cavailles,[a] Oleg A. Filippov,[b] Vincent César,[a] Noël Lugan*[a] and Dmitry A. Valyaev*[a]

[a] Dr. M. Cavailles, Dr. V. César, Dr. N. Lugan, Dr. D. A. Valyaev
LCC-CNRS, Université de Toulouse, CNRS,
205 route de Narbonne 31077 Toulouse, Cedex 4, France
E-mail: noel.lugan@lcc-toulouse.fr, dmitry.valyaev@lcc-toulouse.fr
URL: https://www.lcc-toulouse.fr/dmitry-valyaev/
[b] Dr. O. A. Filippov
A. N. Nesmeyanov Institute of Organoelement Compounds (INEOS),
Russian Academy of Sciences, 28 Vavilov str., GSP-1, B-334, Moscow, 119991, Russia

Supporting information for this article is given via a link at the end of the document.

Abstract: The first manganese complex bearing a chiral *N*-heterocyclic carbene (NHC) ligand was prepared and studied by spectroscopic methods and X-ray diffraction. While IR spectroscopy revealed the existence of two isomers in solution with distinct ν_{CO} band patterns, DFT calculations indicated that these isomers correspond to rotamers around the Mn-NHC bond and their different spectroscopic properties were rationalized by the occurrence of attractive π(C=C)...π*(C≡O) or σ(C−H)...π*(C≡O) intramolecular interligand interactions. The evaluation of this complex in catalytic hydrosilylation of acetophenone using Ph_2SiH_2 under UV irradiation led to the formation of the corresponding (*R*)-alcohol with low enantioselectivity.

Introduction

The use of first row transition metal complexes in catalytic hydrosilylation of multiple carbon-carbon and carbon-heteroatom bonds gained a significant interest from the beginning of 21th century.[1] In that prospect, organometallic manganese compounds occupy one of the leading positions in this area,[2] which can be illustrated by the development in the group of Trovitch of the most active catalysts for C=O bond hydrosilylative reduction of aldehydes,[3] ketones[3] and formates.[4] In sharp contrast to the multitude of identified Mn-based catalytic systems for ketone hydrosilylation, asymmetric version of this transformation remains very scarce. In 2017, Gade mentioned that the Mn(II) alkyl complex **1** supported by a pincer-type bis(oxazolinylmethylidene)isoindoline scaffold (Scheme 1) was capable to reduce acetophenone using various silanes with 70-71% *ee*.[5] In parallel, the group of Huang showed that the Mn(II) dichloride complex **2** (Scheme 1) bearing a bulky iminopyridine-oxazoline ligand was active in hydrosilylation of diverse alkyl(aryl)ketones with $PhSiH_3$ in the presence of $NaBHEt_3$ as activator affording the corresponding alcohols in 80-92% *ee*.[6]

We have previously reported that the half-sandwich Mn(I) complex **3** (Scheme 1) bearing a 1,3-bis(2,4,6-trimethylphenyl)-2*H*-imidazol-2-ylidene (IMes) ligand was active in hydrosilylation of ketones with Ph_2SiH_2 under UV irradiation[7,8] with up to 960 TON achieved for the reduction of 2-acetonaphthone.[7a] Motivated by the performance of this simple catalytic system, we were prompted to investigate structurally similar complexes bearing chiral NHC-type ligands as a possible route to the design of Mn(I) catalysts for asymmetric ketone hydrosilylation. We present herein the synthesis of a half-sandwich Mn(I) complex bearing an enantiopure bicyclic oxazoline-NHC ligand previously developed by Glorius[9] (Scheme 1), its spectroscopic and structural characterization, detailed investigation of its conformational behavior, and preliminary evaluation in catalysis.

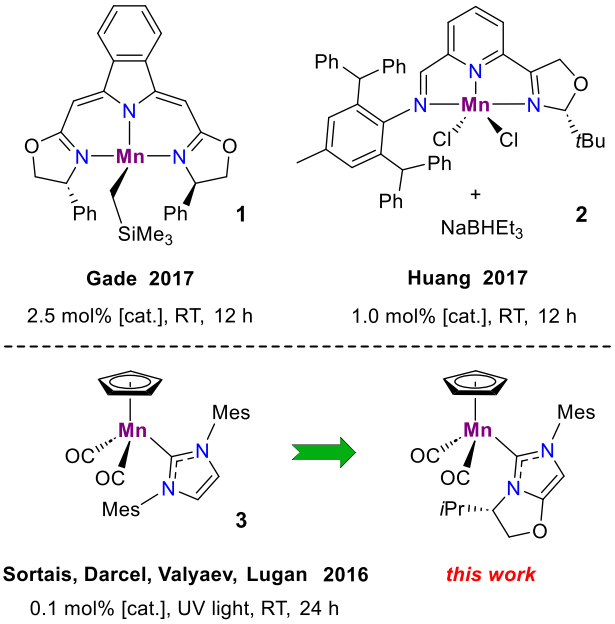

Scheme 1. Known Mn(II) catalysts **1-2** for asymmetric ketone hydrosilylation (top) and proposed chiral upgrade of Mn(I) IMes complex **3** (bottom).

Results and Discussion

The target Mn(I) complex (*S*)-**5** was obtained by photochemical CO ligand substitution in $[CpMn(CO)_3]$ with a free NHC generated *in situ* from the (*S*)-oxazolin[2,3-c]imidazolium salt (*S*)-[**4**]((OTf) and 1.1 equiv. of $KN(SiMe_3)_2$ (KHMDS) in toluene at room temperature (Scheme 2). In contrast to 80-85% yield generally obtained for IMes derivative **3** under similar conditions,[10] the formation of (S)-**5** proceeds in a less efficient manner, which may be related to a lower stability of the free carbene under UV irradiation. Nevertheless, analytically pure product was isolated in *ca.* 40% yield by a combination of column chromatography on silica and crystallization. To the best of our knowledge, complex

(*S*)-**5** represents the first example of manganese complex bearing a chiral NHC ligand.[11,12]

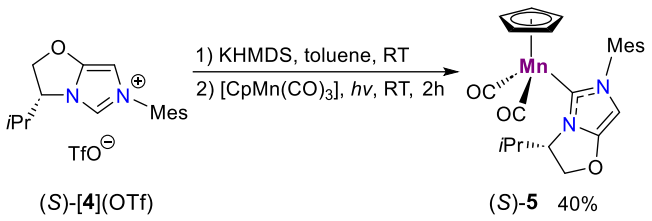

(*S*)-[**4**](OTf) (*S*)-**5** 40%

Scheme 2. Synthesis of Mn(I) complex (*S*)-**5** bearing fused oxazoline-NHC ligand.

^{1}H NMR spectrum of complex (*S*)-**5** in C_6D_6 showed in particular three CH_3 (δ_H 2.14, 2.11, 2.03 ppm) and two aromatic CH (δ_H 6.84, 6.75 ppm) resonances for mesityl group due to the presence of the stereogenic carbon atom; a similar pattern was observed in the ^{13}C NMR spectrum. The backbone NHC proton was observed at δ_H 5.49 ppm, whereas characteristic signals of the oxazoline moiety appeared at δ_H 4.29, 4.11, and 3.91 ppm. The carbene resonance observed at δ_C 193.1 is shielded compared to that of the related IMes complex **3** in the same solvent (δ_C 205.4 ppm).[13] Complex (*S*)-**5** showed two distinct signals for the diastereotopic carbonyl groups at δ_C 235.5 and 234.8 ppm in its ^{13}C NMR spectrum.

The molecular structure of complex (*S*)-**5** obtained by single crystal X-ray diffraction is shown in Figure 1.[14] The compound crystallizes in the chiral $P2_1$ space group and its anticipated (*S*)-absolute configuration was unambiguously confirmed from the X-ray data. The manganese-carbene bond length in (*S*)-**5**, 1.9797(17) Å, is among the shortest ever reported for half-sandwich Mn(I) complexes bearing monodentate NHC ligands (1.981(2)-2.018(3) Å).[10,13,15] The NHC ligand is oriented in an 'eclipsed' conformation mode whereby the [bicyclic] NHC core is almost coplanar with one of the carbonyl ligands, namely C1O1,

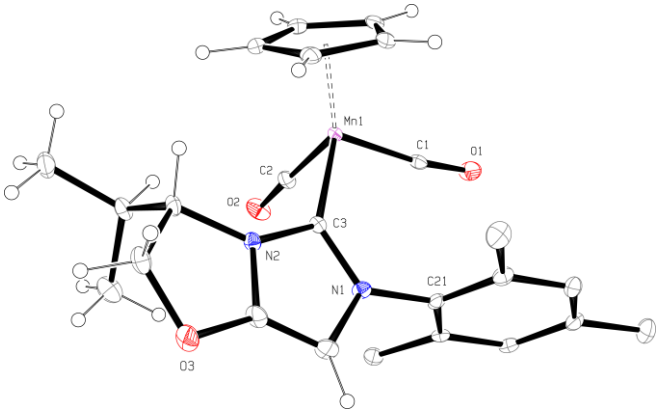

Figure 1. A perspective view of complex **5** (30% probability ellipsoids, hydrogen atoms of mesityl group are omitted for clarity). Selected bond lengths (Å) and angles (°): Mn1−C1 1.7628(18), Mn1−C2 1.7640(18), Mn1−C3 1.9797(17), C4−C5 1.336(3), C1...C21 2.916(1), Mn1−C1−O1 170.90(16), Mn1−C2−O2 177.89(18), N1−C3−Mn1−C1 2.17(2).

with a torsion angle N1−C3−Mn1−C1 of 2.17(2)°. The presence of a short C1...C21 contact 2.916(3) Å inferior to the sum of the corresponding van der Vaals radii (3.2 Å) and the associated bending of the Mn1–C1–O1 fragment (170.90(16)°) are typical features for the occurrence of an intramolecular attractive π(C=C)...π*(C≡O) interaction, as previously identified in half-sandwich Fischer-type[16] and NHC[15a,17] carbene complexes (*vide infra*).

Strikingly, solution IR spectra of complex (*S*)-**5** in various non-polar solvents such as Et_2O, toluene or hexane at room temperature (Figure 2) showed two sets of ν_{CO} bands of almost equal intensity, the difference in average frequency for each pair being of *ca.* 8-10 cm^{-1}. At the same time no dynamic phenomena was evidenced for complex (*S*)-**5** by low temperature ^{1}H NMR spectroscopy (600 MHz, [D_8]-toluene, −80°C, Figure S3). Solid-state IR spectrum of (*S*)-**5** in ATR mode (Figure S4) contained two major ν_{CO} bands at 1899 and 1833 cm^{-1} accompanied with another low intensity pair of peaks at 1914 and 1807 cm^{-1}. While several conformers showing different IR ν_{CO} band patterns have been previously observed for pseudo-octahedral Mn(I) alkoxycarbene [$Cp(CO)_2Mn{=}C(Ph)OAr$][16] and square-planar Ir(I) acyclic diaminocarbene [$Cl(CO)_2Ir(C(NMeAr)_2)$][18] complexes, to the best of our knowledge such spectroscopic particularity was never reported for transition metal NHC complexes.

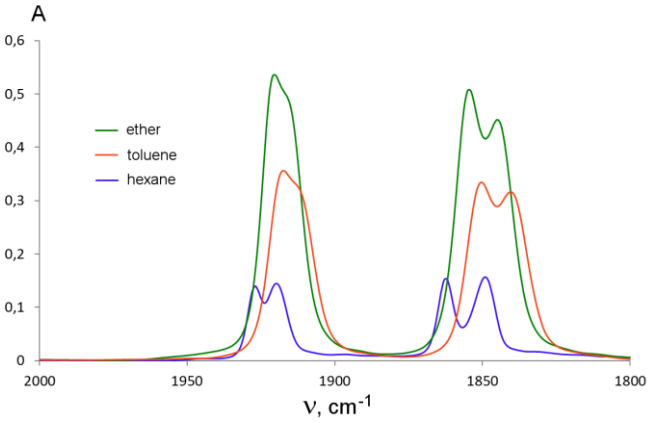

Figure 2. Superposition of solution IR spectra of complex **5** in ether (green), toluene (red) and hexane (blue) at 0.005-0.01 M concentration range. Only 1800-2000 cm^{-1} region of spectra is shown for better clarity.

Taking into account the variation of ν_{CO} frequencies (2-6 cm^{-1}) theoretically predicted for different metal-NHC rotamers of Mn(I) and Fe(II) complexes,[17a] we decided to perform a detailed conformational analysis of complex **5** by DFT calculations using G09/BP86-D3/def2-TZVP method. The geometry optimization revealed the existence of two minima on the potential energy surface corresponding to the conformers **5a** and **5b** (Figure 3) differing by the orientation of bicyclic NHC ligand. The calculated thermodynamic parameters for these species are very close both in gas phase and in solution (see Table S1 for details) being consistent with almost equal ratio observed experimentally. While the geometry of **5a** reproduced well the solid-state structure of complex (*S*)-**5** (torsion angle N1−C3−Mn1−C1 4.82°), in the conformer **5b** the bicyclic NHC ligand is oriented in an alternative 'eclipsed' coordination mode in which the [bicyclic] NHC is rotated by *ca.* 90° around the Mn−$C_{carbene}$ axis, the main core being still almost coplanar with one of the CO ligands (torsion angle N2−C3−Mn1−C2 −80.41°), the mesityl substituent being now away from any of CO ligands. The analysis of calculated IR spectra for **5a** and **5b** (Figure S5) revealed a difference in average ν_{CO} values of *ca.* 13 cm^{-1} in heptane thus perfectly matching with experimental data.

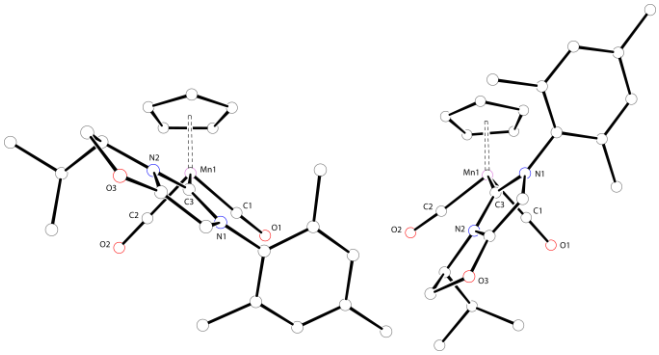

Figure 3. Optimized geometry of conformers **5a** (left) and **5b** (right) differing by NHC ligand orientation (G09/BP86-D3/Def2-TZVP, gas phase, hydrogen atoms are omitted for clarity).

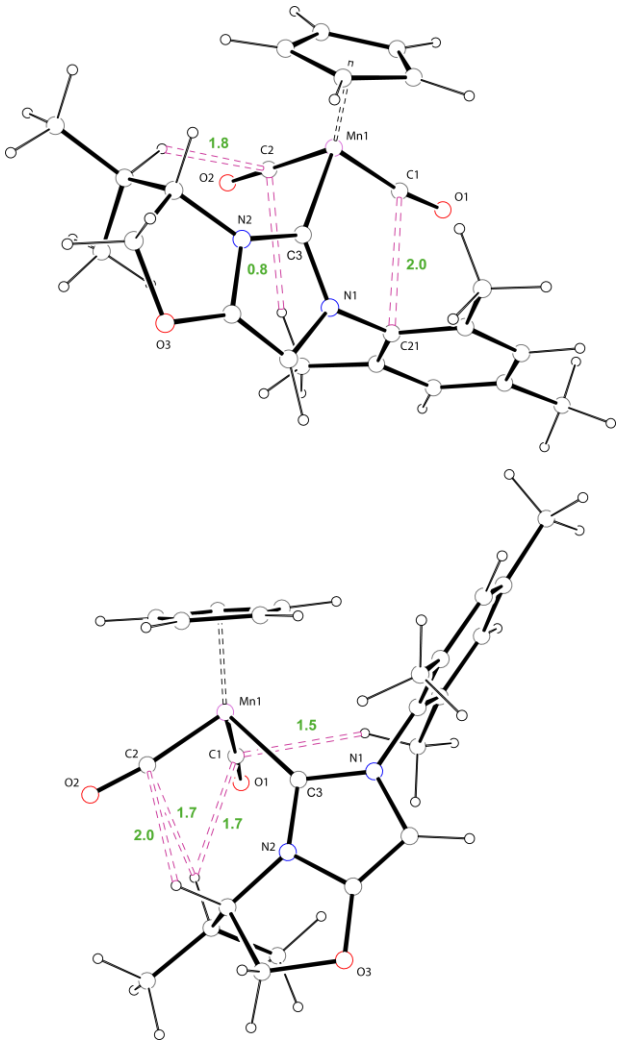

Figure 4. Interligand π(C=C)...π*(C≡O) and σ(C−H)...π*(C≡O) interactions in conformers **5a** (top) and **5b** (bottom) indicated by dotted violet lines. The associated energies E_{int} (kcal/mol) obtained by AIM approach are shown in green.

Surprisingly, it was found that the conformer having lower CO band frequencies is indeed **5b** devoid of any π(C=C)...π*(C≡O) interligand interaction typically leading to a decrease of the corresponding ν_{CO} values.[16,17a] In order to explain this puzzling phenomenon we took a closer look on other weak interligand interactions with carbonyl ligands in both conformers using NBO method[19] and Bader's atoms in molecules (AIM) theory.[20] In case of **5a** besides the anticipated bonding interaction between mesityl group and Mn1−C1−O1 fragment (Figure 4, top), the presence of another type of interaction involving Mn1−C2−O2 moiety was evidenced by the distances of 2.49 and 2.76 Å for the CH of *i*Pr and CH_3 of mesityl, respectively being inferior to the sum of the corresponding van der Waals radii (2.9 Å).[21] NBO analysis (Tables S2) revealed that aryl-to-CO contact results from the occurrence of bonding π(C=C)...π*(C≡O) interactions with total associated energy $\Delta E^{(2)}$ of −1.62 kcal/mol (Figures S6). In agreement with previous results,[21] both C−H...C≡O interactions were rationalized as σ(C−H)...π*(C≡O) interaction (Figure S7, $\Delta E^{(2)}$ −0.72 and −0.19 kcal/mol for CH of *i*Pr and CH_3 of mesityl, respectively) with a contribution of σ*(C−H)...π(C≡O) components (Figure S7, total $\Delta E^{(2)}$ energies −0.26 and −0.21 kcal/mol). All these interligand interactions were also evidenced by the existence of the corresponding bond critical points (Figure S8, Table S3-S5) and their energies E_{int} were estimated by Espinosa-Molins-Lecomte approach[22] to be 2.0, 1.8 and 0.8 kcal/mol, respectively. In case of **5b** four short C−H...C≡O contacts in a range of 2.52-2.55 Å with a participation of both Mn−CO fragments were found (Figure 4, bottom), having the same chemical nature according to NBO analysis (Figure S9) and $\Delta E^{(2)}$ values of *ca.* −0.7 kcal/mol for each one (Table S6). These σ(C−H)...π*(C≡O) interactions were also detected by AIM (Figure S8) and their associated energies E_{int} are situated between 1.5-2.0 kcal/mol (Tables S3-S5).[23] Taking into account generally lower impact of σ(C−H)...π*(C≡O) bonding interactions on the decrease of carbonyl frequencies in transition metal carbene complexes compared to π(C=C)...π*(C≡O) one,[16] we suppose that lower ν_{CO} values observed for the conformer **5b** may be explained by the overall higher number of these interactions.

Finally, complex (*S*)-**5** was tested in hydrosilylation of acetophenone with Ph_2SiH_2 according to previously optimized protocol (1 mol% of catalyst, 1.5 equiv. of silane, UV irradiation, toluene, room temperature).[7b] It was found that irradiation of the reaction mixture over two hours followed by basic hydrolysis led to 95% of substrate conversion with (*R*)-2-phenylethanol being formed as privileged enantiomer in 16% *ee* only. Despite low asymmetric induction, to the best of our knowledge this reaction represents the first half-sandwich NHC complex of 3d transition metal capable to perform asymmetric C=O bond reduction.

Conclusion

We have shown that half-sandwich Mn(I) complex bearing chiral oxazoline-NHC scaffold displays an interesting fluxional behavior in solution allowing the direct observation by IR spectroscopy of two conformers arisen from the NHC ligand rotation across the metal-carbene bond. Spectroscopic properties of these species were rationalized by DFT calculations presuming that a synergy of several σ(C−H)...π*(C≡O) interligand interactions may lead to even higher impact on ν_{CO} frequencies in transition metal carbonyl complexes than a single π(C=C)...π*(C≡O) bonding interaction previously shown to produce stronger C≡O bond elongation.[16] Though the present catalytic system is not efficient for chirality transfer probably due to the lack of rigidity, utilization of bulkier

chiral NHC ligands in structurally similar complexes may be more beneficial.

Experimental Section

General considerations. All manipulations were carried out using standard Schlenk techniques under an atmosphere of dry nitrogen. Dry and oxygen-free organic solvents were obtained using LabSolv (Innovative Technology) solvent purification system. Imidazolium salt (*S*)-[**4**](OTf) was prepared from (*S*)-valinol as previously described,[9,24] all other reagent were used as received. Catalytic hydrosilylation was carried out using a home-made external 15 W light source based on 390 nm LEDs. GC analyses were carried out using a HP 5890 series II gas chromatograph equipped with a flame ionization detector and a Beta DEX 225 capillary column (30 m, 0.25 mm diameter, 0.25 µm thickness). Chromatographic purification of the compounds was performed on silica (0.060-0.200 mm, 60 Å) obtained from Acros Organics flushed with nitrogen just before use. Solution IR spectra were recorded in 0.1 mm CaF_2 cells using a Perkin Elmer Frontier FT-IR spectrometer and given in cm^{-1} with relative intensity in parentheses. ^1H and ^{13}C NMR spectra were obtained on Bruker Avance 400 and Avance 600 spectrometers and referenced to the residual signals of deuterated solvent (^1H and ^{13}C). Elemental analysis was carried out in LCC-CNRS (Toulouse, France) using Perkin Elmer 2400 series II.

Synthesis of complex (*S*)-5. A solution of KHMDS in toluene (0.5 M, 6.6 mL, 3.3 mmol, 1.1 equiv.) was added dropwise at room temperature to a suspension of (*S*)-[**4**](OTf) (1.25 g, 3 mmol, 1.0 equiv.) in toluene (50 mL). The reaction mixture was sonicated during 15 min and the resulting orange solution was transferred by a canula to the photochemical reactor. Solid $[CpMn(CO)_3]$ (612 mg, 3 mmol, 1.0 equiv.) was then added, the solution was further diluted with toluene (150 mL) and irradiated using immersed medium pressure Hg lamp (150 W) under vigorous stirring with periodical IR monitoring. The irradiation was continued until the bands of the product (ν_{CO} 1917, 1850, 1840 cm^{-1}) in solution IR spectra ceased to increase (*ca.* 2 h). The resulting solution was filtered through a short alumina column (neutral, Brockmann type III, 5×2 cm) to remove brown precipitate using toluene as an eluent and evaporated under vacuum. The orange oily residue was purified by column chromatography on silica (10×2 cm) under inert atmosphere. Unreacted $[CpMn(CO)_3]$ was eluted first with hexane as pale yellow band, followed by an orange band of the product (*S*)-**5** eluted with toluene. The eluate was evaporated under vacuum and the residue was recrystallized from ether/hexane mixture to afford complex (*S*)-**5** (520 mg, 40% yield). Single crystals of (*S*)-**5** suitable for X-ray diffraction was obtained from its concentrated solution in toluene at room temperature.

(*S*)-**5:** ^1H NMR (400.1 MHz, C_6D_6, 25°C): δ 6.84 (s, 1H, C*H*$_{Mes}$), 6.75 (s, 1H, C*H*$_{Mes}$), 5.49 (s, 1H, C*H*$_{Im\text{-}4}$), 4.29 (dt, J_{HH} = 7.9 Hz, J_{HH} = 2.6 Hz, 1H, C*H*$_{Ox}$), 4.18 (s, 5H, Cp), 4.10 (dd, J_{HH} = 9.1 Hz, J_{HH} = 2.2 Hz, 1H, CH_{2Ox}), 3.91 (t, J_{HH} = 8.4 Hz, 1H, CH_{2Ox}), 3.16 (septd, J_{HH} = 7.0 Hz, J_{HH} = 2.3 Hz, 1H, C*H*$(CH_3)_2$), 2.14 (s, 3H, $CH_{3\ Mes}$), 2.11 (s, 3H, $CH_{3\ Mes}$), 2.03 (s, 3H, $CH_{3\ Mes}$), 0.69 (d, J_{HH} = 7.0 Hz, 3H, CH(C*H*$_3)_2$), 0.64 ppm (d, J_{HH} = 7.0 Hz, 3H, CH(C*H*$_3)_2$); $^{13}C\{^1H\}$ NMR (100.6 MHz, C_6D_6, 25°C): δ 235.5, 234.8 (Mn–*C*O), 193.1 (Mn−*C*N$_2$), 152.9 (*C*$_{Im\text{-}5}$), 138.9, 138.6, 136.6, 136.2 (*C*$_{Mes}$), 129.4, 129.3 (*C*H$_{Mes}$), 95.6 (*C*H$_{Im\text{-}4}$), 81.9 (Cp), 74.8 (*C*H$_2$ Ox), 61.9 (*C*H$_{Ox}$), 29.5 (*C*H$(CH_3)_2$), 21.1, 18.6 (*C*H$_{3Mes}$), 18.4 (CH(*C*H$_3)_2$), 18.0 (*C*H$_{3Mes}$), 13.8 ppm (CH(*C*H$_3)_2$). IR (toluene): ν_{CO} 1917 (s), 1912 (sh), 1850 (s), 1840 (s), $\nu_{C=C}$ 1663 (m) cm^{-1}. IR (Et_2O): ν_{CO} 1920 (s), 1916 (sh), 1854 (s), 1845 (s), $\nu_{C=C}$ 1664 (m) cm^{-1}. IR (hexane): ν_{CO} 1927 (s), 1920 (s), 1861 (s), 1849 (s), $\nu_{C=C}$ 1657 (m) cm^{-1}. Anal. Found: C, 64.59; H, 6.18; N, 6.12; Calcd. for $C_{24}H_{27}MnN_2O_3$ (M = 446.43) C, 64.57; H, 6.10; N, 6.28.

X-ray diffraction study. X-ray diffraction data were collected on a Bruker D8/APEX II/Incoatec Mo IµS Microsource diffractometer using MoKα radiation (λ = 0.71073 Å, graphite monochromator). All calculations were performed on a PC compatible computer using the WinGX system.[25] The structures were solved using the SIR2018 program,[26] which revealed in each instance the position of most of the non-hydrogen atoms. All the remaining non-hydrogen atoms were located by the usual combination of full matrix least-squares refinement and difference electron density syntheses using the SHELX program.[27] All non-hydrogen atoms were allowed to vibrate anisotropically. The hydrogen atoms were set in idealized positions (R_3CH, C–H = 0.96 Å; R_2CH_2, C–H = 0.97 Å; RCH_3, C–H = 0.98 Å; C(sp^2)–H = 0.93 Å; U_{iso} 1.2 or 1.5 times greater than the Ueq of the carbon atom to which the hydrogen atom is attached) and their positions refined as “riding” atoms.

DFT calculations. Calculations for **5a** and **5b** were performed using the Gaussian 09[28] package with the BP86[29] functional with D3 version of Grimme’s dispersion[30] (DFT/BP86-D3) without any ligand simplification. For all atoms the Def2-TZVP[31] basis set was applied. The structures were optimized without any symmetry restrictions applying ultrafine integration grid and a tight SCF option. Vibrational frequencies were calculates at the same theory level and reported without applying any scaling factors. For NBO analysis complex **5** was divided to three fragments – Cp, $[Mn(CO)_2]$ and oxazoline-NHC ligand and interfragment donations ligand→$[Mn(CO)_2]$ and $[Mn(CO)_2]$→ligand were analysed. The strongest interactions responsible for metal-carbene bonding interactionwere removed from the list (Tables S2 and S6) excluding those with participation of carbene C: and adjacent N atoms. Overlap of certain NBO’s were further visualized by Chemcraft program.[32] Topological analysis of the electron-density distribution function ρ(r) was performed using the *AIMALL*[33] and *Multiwfn v3.6*[34] program packages based on the wave function obtained by the BP86 calculations. The energies of non-covalent interactions were calculated using the correlation between the binding energy (E_{BCP}) and the value of the density-functional potential energy $V_C(r)$ in the corresponding critical point (3, −1): $E = 0.5 \cdot V_C(r)$.[22] Bond ellipticity, ε was defined as $\varepsilon = (\lambda_1/\lambda_2 - 1)$, where λ_1 and λ_2 are the negative eigenvalues of the Hessian of the electron density at the bond critical point ordered such that $\lambda_1 < \lambda_2 < 0$.[20]

Acknowledgements

We thank Centre National de la Recherche Scientifique (CNRS) and Ministry of Science and Higher Education of the Russian Federation (Contract no. 075-03-2023-642) for the support of this work. Computational studies were performed using HPC resources from CALMIP (grant no. P18038).

Keywords: Manganese • N-heterocyclic carbenes • Interligand interactions • Hydrosilylation • DFT calculations

[1] Selected recent reviews: a) L. D. de Almeida, H. Wang, K. Junge, X. Cui, M. Beller, *Angew. Chem. Int. Ed.* **2021**, *60*, 550-565; *Angew. Chem.* **2021**, *133,* 558−573; b) M. Bhunia, P. Sreejyothi, S.K. Mandal, *Coord. Chem. Rev.* **2020**, *405*, 213110; c) B. Royo, *Adv. Organomet. Chem.* **2019**, *72*, 59-102.

[2] a) K. Das, S. Waiba, A. Jana, B. Maji, *Chem. Soc. Rev.* **2022**, *51*, 4386-4464; b) E. S. Gulyaeva, E. S. Osipova, R. Buhaibeh, Y. Canac, J.-B. Sortais, D. A. Valyaev, *Coord. Chem. Rev.* **2022**, *458*, 214421; c) X. Yang, C. Wang, *Chem. Asian J.* **2018**, *13*, 2307-2315; d) R. J. Trovitch, *Acc. Chem. Res.* **2017**, *50*, 2842-2852.

[3] a) C. Ghosh, T. K. Mukhopadhyay, M. Flores, T. L. Groy, R. J. Trovitch, *Inorg. Chem.* **2015**, *54*, 10398-10406; b) T. K. Mukhopadhyay, M. Flores, T. L. Groy, R. J. Trovitch, *J. Am. Chem. Soc.* **2014**, *136*, 882-885.

[4] T. K. Mukhopadhyay, C. L. Rock, M. Hong, D. C. Ashley, T. L. Groy, M.-H. Baik, R. J. Trovitch, *J. Am. Chem. Soc.* **2017**, *139*, 4901-4915.

[5] V. Vasilenko, C. K. Blasius, H. Wadepohl, L. H. Gade, *Angew. Chem. Int. Ed.* **2017**, *56*, 8393-8397; *Angew. Chem.* **2017**, *129*, 8513-8517.

[6] X. Ma, Z. Zuo, G. Liu, Z. Huang, *ACS Omega* **2017**, *2*, 4688-4692.

[7] a) D. A. Valyaev, D. Wei, S. Elangovan, M. Cavailles, V. Dorcet, J.-B. Sortais, C. Darcel, N. Lugan, *Organometallics* **2016**, *35*, 4090-4098; b) J.

Zheng, S. Elangovan, D. A. Valyaev, R. Brousses, V. César, J.-B. Sortais, C. Darcel, N. Lugan, G. Lavigne, *Adv. Synth. Catal.* **2014**, *356*, 1093-1097.

[8] For other examples of hydrosilylation of carbonyl-containing substrates using Mn(I) NHC complexes, see: a) S. Friães, S. Realista, H. Mourão, B. Royo, *Eur. J. Inorg. Chem.* **2022**, *2022*, e202100884; b) H. Mourão, C. S. B. Gomes, S. Realista, B. Royo, *Appl. Organometal. Chem.* **2022**, e6846; c) S. C. A. Sousa, S. Realista, B. Royo, *Adv. Synth. Catal.* **2020**, *362*, 2437-2443; d) M. Pinto, S. Friães, F. Franco, J. Lloret-Fillol, B. Royo, *ChemCatChem* **2018**, *10*, 2734-2740.

[9] F. Glorius, G. Altenhoff, R. Goddard, C. Lehmann, *Chem. Commun.* **2002**, 2704-2705.

[10] A. A. Grineva, D. A. Valyaev, V. César, O. A. Filippov, V. N. Khrustalev, S. E. Nefedov, N. Lugan, *Angew. Chem. Int. Ed.* **2018**, *57*, 7986-7991; *Angew. Chem.* **2018**, *130*, 8118-8123.

[11] a) S. M. P. V. Broeck, C. S. J. Cazin, *Polyhedron* **2021**, *205*, 115204; b) C. Romain, S. Bellemin-Laponnaz, S. Dagorne, *Coord. Chem. Rev.* **2020**, *422*, 213411.

[12] For optically active half-sandwich Mn(I) Fischer-type alkoxycarbene complexes, see: a) K. Weißenbach, H. Fischer, *J. Organomet. Chem.* **2001**, *621*, 344–351; b) H. Fischer, K. Weißenbach, C. Karl, A. Geyer, *Eur. J. Inorg. Chem.* **1998**, 339-347.

[13] D. A. Valyaev, M. A. Uvarova, A. A. Grineva, V. César, S. N. Nefedov, N. Lugan, *Dalton Trans.* **2016**, *45*, 11953-11957.

[14] CCDC 2238406 contains full crystallographic data for the structure of complex (*S*)-**5**. These data can be obtained free of charge from the Cambridge Crystallographic Data Centre via www.ccdc.cam.ac.uk/data_request/cif.

[15] a) R. Brousses, V. Maurel, J.-M. Mouesca, V. César, N. Lugan, D. A. Valyaev, *Dalton Trans.* **2021**, *50*, 14264-14272; b) M. Batool, T. A. Martin, A. G. Algarra, M. W. George, S. A. Macgregor, M. F. Mahon, M. K. Whittlesey, *Organometallics* **2012**, *31*, 4971-4979; c) R. Fraser, P. H. van Rooyen, J. de Lange, I. Cukrowski, M. Landman, *J. Organomet. Chem.* **2017**, *840*, 11-22.

[16] D. A. Valyaev, R. Brousses, N. Lugan, I. Fernandez, M. A. Sierra, *Chem. Eur. J.* **2011**, *17*, 6602-6605.

[17] a) A. A. Grineva, O. A. Filippov, Y. Canac, J.-B. Sortais, S. E. Nefedov, N. Lugan, V. César, D. A. Valyaev, *Inorg. Chem.* **2021**, *60*, 4015-4025; b) V. César, L. C. Misal Castro, T. Dombray, J.-B. Sortais, C. Darcel, S. Labat, K. Miqueu, J.-M. Sotiropoulos, R. Brousses, N. Lugan, G. Lavigne, *Organometallics* **2013**, *32*, 4643-4655.

[18] M. S. Collins, E. L. Rosen, V. M. Lynch, C. W. Bielawski, *Organometallics* **2010**, *29*, 3047-3053.

[19] *NBO 6.0.* E. D. Glendening, J. K. Badenhoop, A. E. Reed, J. E. Carpenter, J. A. Bohmann, C. M. Morales, C. R. Landis, F. Weinhold, Theoretical Chemistry Institute, University of Wisconsin, Madison, **2013**.

[20] a) R. F. W. Bader, *Atoms in Molecules: A Quantum Theory*, Oxford University Press, **1994**; b) P. L. Popelier, *Atoms in Molecules: An Introduction*, Prentice Hall, London, **2000**; c) C. Matta, R. J. Boyd, *Quantum Theory of Atoms in Molecules: Recent Progress in Theory and Application*, Wiley-VCH: New York, **2007**.

[21] N. Lugan, I. Fernandez, R. Brousses, D. A. Valyaev, G. Lavigne, N. A. Ustynyuk, *Dalton Trans.* **2013**, *42*, 898-901 and references therein.

[22] a) E. Espinosa, I. Alkorta, I. Rozas, J. Elguero, E. Molins, *Chem. Phys. Lett.* **2001**, *336*, 457-461; b) E. Espinosa, E. Molins, C. Lecomte, *Chem. Phys. Lett.* **1998**, *285*, 170-173.

[23] Several weak C−H...H−C interactions with estimated E_{int} in a range of 0.7-1.4 kcal/mol were also detected by AIM in both conformers **5a** and **5b** (see Figure S10 and Table S5 for details). While these contacts may contribute in part for the stabilization of both species, they should not influence ν_{CO} band frequencies and therefore not discussed herein.

[24] J. Seeyad, P. K. Patra, Y. Zhang, J. Y. Ying, *Org. Lett.* **2008**, *10*, 953-956.

[25] L. J. Farrugia, *J. Appl. Crystallogr.* **2012**, *45*, 849-854.

[26] M. C. Burla, R. Caliandro, B. Carrozzini, G. L. Cascarano, C. Cuocci, C. Giacovazzo, M. Mallamo, A. Mazzone, G. Polidori, *J. Appl. Cryst.* **2015**, *48*, 306-309.

[27] G. M. Sheldrick, *Acta Crystallogr.* **2015**, *A71*, 3-8.

[28] M. J. Frisch, G. W. Trucks, H. B. Schlegel, G. E. Scuseria, M. A. Rob, J. R. Cheeseman, J. A. M. Jr., T. Vreven, K. N. Kudin, J. C. Burant, J. M. Millam, S. S. Iyengar, J. Tomasi, V. Barone, B. Mennucci, M. Cossi, G. Scalmani, N. Rega, G. A. Petersson, H. Nakatsuji, M. Hada, M. Ehara, K. Toyota, R. Fukuda, J. Hasegawa, M. Ishida, T. Nakajima, Y. Honda, O. Kitao, H. Nakai, M. Klene, X. Li, J. E. Knox, H. P. Hratchian, J. B. Cross, V. Bakken, C. Adamo, J. Jaramillo, R. Gomperts, R. E. Stratmann, O. Yazyev, A. J. Austin, R. Cammi, C. Pomelli, J. W. Ochterski, P. Y. Ayala, K. Morokuma, G. A. Voth, P. Salvador, J. J. Dannenberg, V. G. Zakrzewski, S. Dapprich, A. D. Daniels, M. C. Strain, O. Farkas, D. K. Malick, A. D. Rabuck, K. Raghavachari, J. B. Foresman, J. V. Ortiz, Q. Cui, A. G. Baboul, S. Clifford, J. Cioslowski, B. B. Stefanov, G. Liu, A. Liashenko, P. Piskorz, I. Komaromi, R. L. Martin, D. J. Fox, T. Keith, M. A. Al-Laham, C. Y. Peng, A. Nanayakkara, M. Challacombe, P. M. W. Gill, B. Johnson, W. Chen, M. W. Wong, C. Gonzalez, J. A. Pople, *Gaussian, Inc.*, Wallingford, CT, **2009**.

[29] a) A. D. Becke, *Phys. Rev. A* **1988**, *38*, 3098-3100; b) J. P. Perdew, *Phys. Rev. B* **1986**, *33*, 8822-8824.

[30] S. Grimme, J. Antony, S. Ehrlich, H. Krieg, *J. Chem. Phys*. **2010**, *132*, 154104.

[31] a) b) F. Weigend, *Phys. Chem. Chem. Phys.* **2006**, *8*, 1057-1065; b) F. Weigend, R. Ahlrichs, *Phys. Chem. Chem. Phys.* **2005**, *7*, 3297-3305.

[32] *Chemcraft* - graphical software for visualization of quantum chemistry computations. https://www.chemcraftprog.com

[33] *AIMAll* (Version 19.10.12), T. A. Keith, TK Gristmill Software, Overland Park KS, USA, **2019** (aim.tkgristmill.com).

[34] T. Lu, F. Chen, *J. Comput. Chem.* **2012**, *33*, 580-592.